Available online at www.sciencedirect.com
SCIENCE DIRECT®
Journal of Sound and Vibration 274 (2004) 863–875
JOURNAL OF SOUND AND VIBRATION
www.elsevier.com/locate/jsvi

Dynamic modelling and control of a rotating Euler–Bernoulli beam

J.B. Yang*, L.J. Jiang, D.CH. Chen

Department of Mechanics and Engineering Science, Peking University, Beijing 100871, People's Republic of China

Received 24 January 2003; accepted 5 June 2003

Abstract

Flexible motion of a uniform Euler–Bernoulli beam attached to a rotating rigid hub is investigated. Fully coupled non-linear integro-differential equations, describing axial, transverse and rotational motions of the beam, are derived by using the extended Hamilton's principle. The centrifugal stiffening effect is included in the derivation. A finite-dimensional model, including couplings of axial and transverse vibrations, and of elastic deformations and rigid motions, is obtained by the finite element method. By neglecting the axial motion, a simplified modelling, suitable for studying the transverse vibration and control of a beam with large angle and high-speed rotation, is presented. And suppressions of transverse vibrations of a rotating beam are simulated with the model by combining positive position feedback and momentum exchange feedback control laws. It is indicated that an improved performance for vibration control can be achieved with the method.

1. Introduction

Recently, the problem of modelling and controling a rotating flexible beam has been given widespread attention due to practical applications such as flexible robot arms, helicopter rotor blades, turbine machine rotor blades, and spacecrafts with flexible appendages.

A rotating beam differs from a non-rotating beam in having coupling of elastic deformations and rigid-body motions. The importance of the coupling was observed by Yigit et al. [1] for Euler–Bernoulli beams, and Naganathan and Soni [2] for Timoshenko beams. Dynamic modellings of rotating beam system, neglected the influence of the centrifugal force on transverse deformations, were studied by Hunagud and Sarkar [3], Baruh and Tadikonda [4] and Choura et al. [5] for

*Corresponding author. Tel.: 86-10-62751816.
E-mail address: jbyang@mail.mech.pku.edu.cn (J.B. Yang).

0022-460X/$ - see front matter © 2003 Elsevier Ltd. All rights reserved.
doi:10.1016/S0022-460X(03)00611-4

Euler–Bernoulli beams, and Kane et al. [6] and Simo and Vu-Quoc [7,8] for Timoshenko beams. Considering the centrifugal stiffening effect, Yigit et al. [1] and Bloch [9] derived the coupling equations of motion of flexible beam and rigid body. Rotating beams with tip mass were studied by Zhu and Mote [10] for Euler–Bernoulli beams, and by Yuan and Hu [11] for Timoshenko beams with the effect of centrifugal stiffening. Except that in Ref. [5], though not including the stiffening effect, all the models above neglect the axial motion of the beam.

Dynamic behaviors of rotating beam have been investigated by various researchers. Putter and Manor [12] used the finite element method (FEM) to study the natural frequencies of a rotating beam. Hoa [13] and Khulief [14] did a similar work, but including a tip mass for a uniform beam and a taper beam. Wright et al. [15] investigated the vibration modes and natural frequencies using the Frobenius method. Du et al. [16] did a similar study for a Timoshenko beam. In Ref. [1], the extended Galerkin method was used to study the effects of the coupling terms upon the vibration waveforms.

Because of the coupling of flexible deformations and rigid motions, the problem of transverse vibrations control of rotating beams is more complicated than that of non-rotating beams. Usually, Euler–Bernoulli beam theory is applied in their controller design and the assumed modes method is used to obtain the discretized finite-dimensional dynamic model of vibration control [10,11]. Some techniques, such as the optimal control [10,11], shear force feedback control [17], and sliding modes control [18], have been used to the suppression of vibrations. But if employing the coupling of transverse flexible deformations and rigid motions, a concept of controlling the attitude of the rigid hub can be introduced to suppress the transverse vibration of the beam. The so-called momentum exchange feedback (MEF) control is such a technique [19]. By combining this technique with other control methods, such as the positive position feedback (PPF) [20], the suppression of vibration can be gained dramatically.

In this paper, fully coupled non-linear integro-differential equations, describing axial, transverse and rotational motions of a rotating uniform Euler–Bernoulli beam, are derived by using the extended Hamilton's principle. The centrifugal stiffening effect is included in the derivation. A finite-dimensional model, including couplings of axial and transverse vibrations, and of flexible deformations and rigid motions, is obtained by the FEM. A simplified FEM model, suitable for studying transverse vibration and control of a beam with large angle and high-speed rotation, is presented by neglecting the axial motion. And with the model, suppressions of the transverse vibrations of a rotating beam, by applying the PPF to the beam and the MEF to the rigid hub, are simulated. Numerical results indicate excellent performance of suppression can be achieved with such method.

2. Non-linear dynamic modelling

As depicted schematically in Fig. 1, a uniform Euler–Bernoulli beam of length L, area moment inertia I, cross-sectional area A, density ρ and Young's modulus E, is attached to a rigid hub of radius R and mass moment of inertia I_h, which in turn is connected to an actuator that supplies torque $\tau(t)$ and rotates about the axis perpendicular to the plane $X'-Y'$. Flexible deformations of the beam are described in a reference co-ordinate OXY, which rotates relative to the inertia

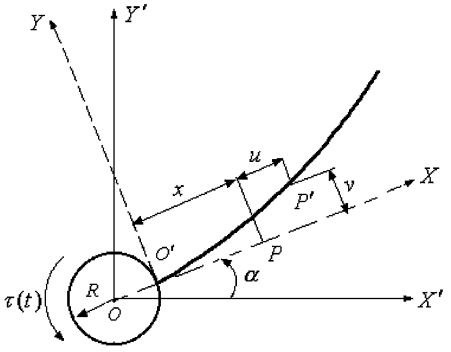

Fig. 1. Hub–beam system.

co-ordinate $O'X'Y'$ by $\alpha(t)$. The X-axis is tangential to the neutral axis of the beam at the point of attachment of the beam to the rigid.

The motion of the beam is restricted to the horizontal X–Y plane, and the gravitational force is of no consideration. The axial and transverse displacements of the beam are denoted by u and v, respectively. Large overall rotation $\alpha(t)$ and high angular speed $\dot{\alpha}(t)$ are permitted; so couplings between the rigid-body and elastic motions occur in the following model.

A material point P, on the neutral axis X of the beam in natural condition, moves to point P' under deformations. The position vector at the point P' on the deformed neutral axis can be expressed as

$$\vec{r}(x,t) = (R + x + u)\vec{i} + v(x,t)\vec{j}, \tag{1}$$

where $\vec{i}$ and $\vec{j}$ are the unit vectors along OX and OY in the inertia co-ordinate, respectively. Then the inertia velocity of P' on the beam is

$$\dot{\vec{r}} = (\dot{u} - v\dot{\alpha})\vec{i} + [(R + x + u)\dot{\alpha} + \dot{v}]\vec{j}, \tag{2}$$

where $(^{\bullet})$ denotes the time derivative. So the kinetic energy of the system can be written as

$$T = \tfrac{1}{2}\rho A \int_0^L \dot{\vec{r}} \cdot \dot{\vec{r}}\, \mathrm{d}x + \tfrac{1}{2} I_h \dot{\alpha}^2. \tag{3}$$

The potential energy of the system consists of two parts, the elastic potential energy and the potential energy arising from the centrifugal force. By the assumption that the beam is linearly elastic and deformation is small the potential energy is

$$V = \tfrac{1}{2} EA \int_0^L u'^2\, \mathrm{d}x + \tfrac{1}{2} EI \int_0^L v''^2\, \mathrm{d}x + \tfrac{1}{2}\rho A \int_0^L F v'^2\, \mathrm{d}x, \tag{4}$$

where $()'$ denotes partial differentiation with respect to x, and F is the force due to rotation-induced axial centrifugal force. The force F can be expressed as

$$F = \rho A \int_x^L \dot{\alpha}^2 [R + \zeta]\, \mathrm{d}\zeta = \rho A \dot{\alpha}^2 \left[R(L - x) + \tfrac{1}{2}(L^2 - x^2)\right]. \tag{5}$$

Then, the Lagrangian function of the system can be written as

$$\begin{aligned}\Psi = T - V &= \int_0^L \Phi(u, u'; v, v', v'', \dot{v}, v; \dot{\alpha})\,\mathrm{d}x \\ &= \int_0^L \{\tfrac{1}{2}\rho A\{(\dot{u} - v\dot{\alpha})^2 + [(R + x + u)\dot{\alpha} + \dot{v}]^2\} - \tfrac{1}{2}EAu'^2 - \tfrac{1}{2}EIv''^2 \\ &\quad - \tfrac{1}{2}\rho A\dot{\alpha}^2[R(L - x) + \tfrac{1}{2}(L^2 - x^2)]v'^2\}\,\mathrm{d}x + \tfrac{1}{2}I_h\dot{\alpha}^2, \end{aligned} \tag{6}$$

where $\Phi(u, u'; v, v', v'', \dot{v}; \dot{\alpha})$ is the Lagrangian density function. And the virtual work done δW by external torque $\tau(t)$ at the hub is given by

$$\delta W = \tau(t)\delta\alpha. \tag{7}$$

Substituting Eqs. (3), (4) and (7) into the extended Hamilton's principle, $\int_{t_1}^{t_2}(\delta T - \delta V + \delta W)\,\mathrm{d}t = 0$, taking the variations with respect to the elastic deformations u and v, and (the rotation angle) α, yields governing equations of motion and the corresponding boundary conditions. They are

$$\rho A[\ddot{u} - 2\dot{\alpha}\dot{v} - \ddot{\alpha}v - \dot{\alpha}^2(R + x + u)] - EAu'' = 0, \tag{8}$$

$$\begin{aligned}&\rho A[\ddot{v} + 2\dot{\alpha}\dot{u} - \dot{\alpha}^2 v + \ddot{\alpha}(R + x + u)] + EIv''''\\ &\quad - \rho A\dot{\alpha}^2\{[R(L - x) + \tfrac{1}{2}(L^2 - x^2)]v'' - (R + x)v'\} = 0,\end{aligned} \tag{9}$$

$$\begin{aligned}&I_h\ddot{\alpha} + \left\{\rho A\int_0^L \{v^2 + (R + x + u)^2 - [R(L - x) + \tfrac{1}{2}(L^2 - x^2)]v'^2\}\,\mathrm{d}x\right\}\ddot{\alpha}\\ &\quad + \left\{\rho A\int_0^L \{2v\dot{v} + 2(R + x + u)\dot{u} - 2[R(L - x) + \tfrac{1}{2}(L^2 - x^2)]v'\dot{v}'\}\,\mathrm{d}x\right\}\dot{\alpha}\\ &\quad + \rho A\int_0^L [(R + x + u)\ddot{v} - \ddot{u}v]\,\mathrm{d}x = \tau(t),\end{aligned} \tag{10}$$

with the corresponding boundary conditions

$$u(0) = 0, \quad v(0) = 0, \quad v'(0) = 0, \tag{11}$$

and

$$u'(L) = 0, \quad v''(L) = 0, \quad v'''(L) = 0. \tag{12}$$

Eqs. (8)–(10) include non-linear couplings of the axial elastic deformation u, the transverse elastic deformation v, and the hub rotation angle α. If vanishing some terms of Eqs. (9) and (10), the non-linear model (8)–(10) can be simplified to the model described by Eqs. (24)–(26) in Ref. [5]. The reason of resulting in such differences is that the potential energy, arising from the rotation-induced axial centrifugal force, was not included in the total system energy in Ref. [5].

Neglecting the axial displacement u, that is setting $u = 0$ in Eqs. (9) and (10), yields the following equations:

$$\begin{aligned}&\rho A[\ddot{v} - \dot{\alpha}^2 v + \ddot{\alpha}(R + x)] + EIv''''\\ &\quad - \rho A\dot{\alpha}^2\{[R(L - x) + \tfrac{1}{2}(L^2 - x^2)]v'' - (R + x)v'\} = 0,\end{aligned} \tag{13}$$

$$I_h\ddot{\alpha} + \left\{\rho A \int_0^L \{v^2 + (R+x)^2 - [R(L-x) + \tfrac{1}{2}(L^2 - x^2)]v'^2\}\,\mathrm{d}x\right\}\ddot{\alpha}$$
$$+ \left\{\rho A \int_0^L \{2v\dot{v} - 2[R(L-x) + \tfrac{1}{2}(L^2 - x^2)]v'\dot{v}'\}\,\mathrm{d}x\right\}\dot{\alpha}$$
$$+ \rho A \int_0^L [(R+x)\ddot{v}]\,\mathrm{d}x = \tau(t). \tag{14}$$

The boundary conditions are the same as those in Eqs. (11) and (12). The governing differential equations above are used frequently in control applications, and they also can be got from Refs. [1,9] directly, and from Refs. [11,12] by some steps of simplification.

3. Finite-dimensional non-linear modelling

In this part, the finite-dimensional non-linear modelling is obtained following the idea of Stylianou and Tabarrok [21] used for developing the finite-dimensional modelling of an axially moving beam.

3.1. Finite element discretization

In order to develop the finite element equations for the beam element, the beam is divided into n elements of equal length l. As shown in Fig. 2, the location of a point A along the neutral axis of the ith element in the element co-ordinate $\overline{oxy}$, with respect to the reference co-ordinate OXY, can be expressed as

$$x = L_i + \bar{x}, \tag{15}$$

where

$$L_i = (i-1)\frac{L}{n}. \tag{16}$$

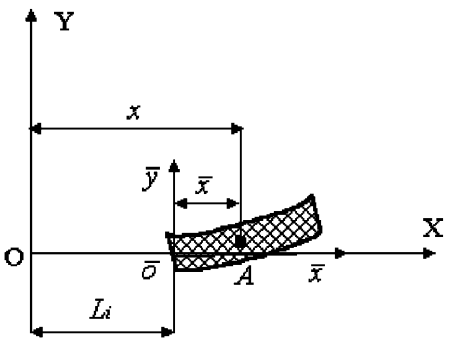

Fig. 2. The element co-ordinate system.

Then the Lagrangian function for the ith element is given by

$$\Psi_i = \int_0^l \{\tfrac{1}{2}\rho A\{(\dot{u} - v\dot{\alpha})^2 + [(R + L_i + \bar{x} + u)\dot{\alpha} + \dot{v}]^2\} - \tfrac{1}{2}EAu'^2 - \tfrac{1}{2}EIv''^2 - \tfrac{1}{2}\rho A\dot{\alpha}^2[R(L - L_i - \bar{x}) + \tfrac{1}{2}(L + L_i + \bar{x})(L - L_i - \bar{x})]\bar{v}'^2\}\,\mathrm{d}\bar{x}. \tag{17}$$

For simplicity, the overbars in the above equations are dropped in the following analyses.

From the theory of the FEM [22], we have

$$u = [N]_u\{u\}, \quad v = [N]_v\{v\}, \tag{18}$$

where $[N]_u$ and $\{u\}$ are the shape function and nodal variables vector of axial displacement, respectively; and $[N]_v$ and $\{v\}$ are those of the transverse displacement. $[N]_u$ and $[N]_v$ can be expressed as

$$[N]_u = \left[1 - \frac{x}{l} \quad \frac{x}{l}\right],$$
$$[N]_v = \left[1 - \frac{3x^2}{l^2} + \frac{2x^3}{l^3} \quad x - \frac{2x^2}{l} + \frac{x^3}{l^2} \quad \frac{3x^2}{l^2} - \frac{2x^3}{l^3} \quad -\frac{x^2}{l} + \frac{x^2}{l^2}\right]. \tag{19}$$

Vectors $\{u\}$ and $\{v\}$ are

$$\{u\}^{\mathrm{T}} = [u_1 \quad u_2], \quad \{v\}^{\mathrm{T}} = [v_1 \quad \theta_1 \quad v_2 \quad \theta_2], \tag{20}$$

where u_1 is the axial nodal displacement , and v_1 and θ_1 are the transverse nodal displacement and slope variables of the left-hand end of the element, respectively, and u_2, v_2 and θ_2 are those of the right-hand end of the element. From Eq. (18), then have

$$u' = [N]'_u\{u\}, \quad \dot{u} = [N]_u\{\dot{u}\}; \tag{21}$$

$$v' = [N]'_v\{v\}, \quad v'' = [N]''_v\{v\}, \quad \dot{v} = [N]_v\{\dot{v}\}. \tag{22}$$

Substituting Eqs. (18), (21) and (22) into Eq. (17), we obtain

$$\Psi_i = \tfrac{1}{2}\{\dot{u}\}^{\mathrm{T}}[m]_u\{\dot{u}\} - \tfrac{1}{2}\{u\}^{\mathrm{T}}[k]_u\{u\} + \tfrac{1}{2}\dot{\alpha}^2\{u\}^{\mathrm{T}}[k]_{u1}\{u\} + \dot{\alpha}^2[k]_{u2}\{u\} - \dot{\alpha}\{\dot{u}\}^{\mathrm{T}}[c]_{uv}\{v\} + \tfrac{1}{2}\{\dot{v}\}^{\mathrm{T}}[m]_v\{\dot{v}\} - \tfrac{1}{2}\{v\}^{\mathrm{T}}[k]_v\{v\} + \tfrac{1}{2}\dot{\alpha}^2\{v\}^{\mathrm{T}}[k]_{v1}\{v\} - \tfrac{1}{2}\dot{\alpha}^2\{v\}^{\mathrm{T}}[k]_{v2}\{v\} + \dot{\alpha}\{\dot{v}\}^{\mathrm{T}}[c]_{vu}\{u\} + \dot{\alpha}[c]_v\{\dot{v}\} + \tfrac{1}{2}I_b\dot{\alpha}^2, \tag{23}$$

where

$$[m]_u = \int_0^l \rho A[N]_u^{\mathrm{T}}[N]_u\,\mathrm{d}x, \quad [m]_v = \int_0^l \rho A[N]_v^{\mathrm{T}}[N]_v\,\mathrm{d}x, \tag{24, 25}$$

$$[k]_u = \int_0^l EA[N]_u'^{\mathrm{T}}[N]'_u\,\mathrm{d}x, \quad [k]_v = \int_0^l EI[N]_v''^{\mathrm{T}}[N]''_v\,\mathrm{d}x, \tag{26, 27}$$

$$[k]_{u1} = \int_0^l \rho A[N]_u^{\mathrm{T}}[N]_u\,\mathrm{d}x, \quad [k]_{v1} = \int_0^l \rho A[N]_v^{\mathrm{T}}[N]_v\,\mathrm{d}x, \tag{28, 29}$$

$$[k]_{u2} = \int_0^l \rho A(R + L_i + x)[N]_u\,\mathrm{d}x, \tag{30}$$

$$[k]_{v2} = \int_0^l \rho A[R(L - L_i - x) + \tfrac{1}{2}(L + L_i + x)(L - L_i - x)][N]_v'^{\mathrm{T}}[N]_v' \,\mathrm{d}x, \tag{31}$$

$$[c]_{uv} = \int_0^l \rho A[N]_u^{\mathrm{T}}[N]_v \,\mathrm{d}x, \quad [c]_{vu} = \int_0^l \rho A[N]_v^{\mathrm{T}}[N]_u \,\mathrm{d}x, \tag{32, 33}$$

$$[c]_v = \int_0^l \rho A(R + L_i + x)[N]_v \,\mathrm{d}x, \quad I_b = \rho A \int_0^l (R + L_i + x)^2 \,\mathrm{d}x. \tag{34, 35}$$

The matrices $[m]_u$ and $[m]_v$ correspond to the well-known consistent mass matrices of the beam element of axial and transverse vibrations, respectively, whereas $[k]_u$ and $[k]_v$ are the stiffness matrices. Their components can be found in books on finite element, e.g., Ref. [22]. The other matrices can be determined by using a symbolic-computation program.

3.2. The Lagrange equation implement

The Lagrange equations for an element are given by

$$\frac{\partial \Psi_i}{\partial \{u\}^{\mathrm{T}}} - \frac{\mathrm{d}}{\mathrm{d}t}\left[\frac{\partial \Psi_i}{\partial \{\dot{u}\}^{\mathrm{T}}}\right] = \{0\}, \tag{36}$$

$$\frac{\partial \Psi_i}{\partial \{v\}^{\mathrm{T}}} - \frac{\mathrm{d}}{\mathrm{d}t}\left[\frac{\partial \Psi_i}{\partial \{\dot{v}\}^{\mathrm{T}}}\right] = \{0\}, \tag{37}$$

$$\frac{\partial \Psi_i}{\partial \alpha} - \frac{\mathrm{d}}{\mathrm{d}t}\left[\frac{\partial \Psi_i}{\partial \dot{\alpha}}\right] = \tau(t). \tag{38}$$

Evaluating required quantities in the Eqs. (36)–(38), and substituting the results into the Lagrange function (23), we obtain the element governing equations as

$$[m]_u\{\ddot{u}\} - 2\dot{\alpha}[c]_{uv}\{\dot{v}\} + ([k]_u - \dot{\alpha}^2[k]_{u1})\{u\} - \ddot{\alpha}[c]_{uv}\{v\} = \dot{\alpha}^2[k]_{u2}^{\mathrm{T}}, \tag{39}$$

$$[m]_v\{\ddot{v}\} + 2\dot{\alpha}[c]_{vu}\{\dot{u}\} + ([k]_v - \dot{\alpha}^2[k]_{v1} + \dot{\alpha}^2[k]_{v2})\{v\} + \ddot{\alpha}[c]_{vu}\{u\} = -\ddot{\alpha}[c]_v^{\mathrm{T}}, \tag{40}$$

$$\begin{aligned} m_\alpha\ddot{\alpha} + k_\alpha\dot{\alpha} - \{\ddot{u}\}^{\mathrm{T}}[c]_{uv}\{v\} - \{\dot{u}\}^{\mathrm{T}}[c]_{uv}\{\dot{v}\} \\ + \{\ddot{v}\}^{\mathrm{T}}[c]_{vu}\{u\} + \{\dot{v}\}^{\mathrm{T}}[c]_{vu}\{\dot{u}\} + [c]_v\{\ddot{v}\} = \tau, \end{aligned} \tag{41}$$

where

$$m_\alpha = I_b + \{u\}^{\mathrm{T}}[k]_{u1}\{u\} + 2[k]_{u2}\{u\} + \{v\}^{\mathrm{T}}([k]_{v1} - [k]_{v2})\{v\}, \tag{42}$$

$$k_\alpha = 2\{\dot{u}\}^{\mathrm{T}}[k]_{u1}\{u\} + 2[k]_{u2}\{\dot{u}\} + 2\{\dot{v}\}^{\mathrm{T}}([k]_{v1} - [k]_{v2})\{v\}. \tag{43}$$

In the derivation, we have used the identity $[c]_{uv} = [c]_{vu}^{\mathrm{T}}$. Assembly of the element equations (39)–(43) to develop global equations and the global equations can be expressed as

$$[M]_u\{\ddot{u}\} - 2\dot{\alpha}[C]_{uv}\{\dot{v}\} + ([K]_u - \dot{\alpha}^2[K]_{u1})\{u\} - \ddot{\alpha}[C]_{uv}\{v\} = \{\dot{\alpha}^2[K]_{u2}^{\mathrm{T}}\}, \tag{44}$$

$$[M]_v\{\ddot{v}\} + 2\dot{\alpha}[C]_{vu}\{\dot{u}\} + ([K]_v - \dot{\alpha}^2[K]_{v1} + \dot{\alpha}^2[K]_{v2})\{v\} + \ddot{\alpha}[C]_{vu}\{u\} = \{-\ddot{\alpha}[C]_v^{\mathrm{T}}\}, \tag{45}$$

$$M_\alpha\ddot{\alpha} + K_\alpha\dot{\alpha} - \{\ddot{u}\}^{\mathrm{T}}[C]_{uv}\{v\} - \{\dot{u}\}^{\mathrm{T}}[C]_{uv}\{\dot{v}\} + \{\ddot{v}\}^{\mathrm{T}}[C]_{vu}\{u\} + \{\dot{v}\}^{\mathrm{T}}[C]_{vu}\{\dot{u}\} + [C]_v\{\ddot{v}\} = \tau. \quad (46)$$

The equations above are a set of non-linear, coupled secondorder differential equations. If the axial deformation is neglected, the above equations can be written as

$$[M]_v\{\ddot{v}\} + [K]_v\{v\} + \dot{\alpha}^2(-[K]_{v1} + [K]_{v2})\{v\} = \{-\ddot{\alpha}[C]_v^{\mathrm{T}}\}, \quad (47)$$

$$[I_h + I_b + \{v\}^{\mathrm{T}}([K]_{v1} - [K]_{v2})\{v\}]\ddot{\alpha} + 2[\{\dot{v}\}^{\mathrm{T}}([K]_{v1} - [K]_{v2})\{v\}]\dot{\alpha} + [C]_v\{\ddot{v}\} = \tau. \quad (48)$$

It should be indicated that in Eq. (48), moment inertia of the rigid hub I_h has been included in the global mass matrix. Eqs. (47) and (48) can be used to study the dynamic behaviors and vibration control of rotating Euler–Bernoulli beams. The following simulations of suppressing transverse vibrations of a rotating beam are based on these two equations.

4. Active vibration control

The use of piezoelectric sensors and/or actuators, embedded in materials or surface bonded on structures, has attracted considerable interest for the vibration control of flexible structures. In order to avoid the notorious problem of "spillover", PPF control law is popularly used for suppressing the vibrations. But such method has the localization of having a small control gain, which must be below 1 [20]. This small gain weakens the performance of vibration suppression of flexible structures.

Employing the coupling of transverse flexible deformations and rigid motions, a concept of controlling the attitude of the rigid body, can be introduced to suppress the transverse vibrations of rotating beam. The so-called MEF control is one of the techniques [19]. By combining PPF and MEF, the performance of PPF control can be improved in suppressing transverse vibrations of rotating beam, and dramatic results can be gained.

In the following simulating work for suppressing vibrations of a rotating beam, only one pair of piezoelectric sensor/actuator is used and surface bonded at the root of the beam. PPF control law is applied to the root of the beam by piezoelectric actuator, and MEF control is applied to the rigid hub by DC servomotor. Root shear force and bending moment of the flexible beam are measured by piezoelectric sensor.

4.1. Modelling of vibration control

In Section 3, the finite-dimensional equations, expressing coupling of transverse vibrations of flexible beam and rigid-body motions, have been given by Eqs. (47) and (48) by neglecting the axial motion in Eqs. (44)–(46). But if not considering effects of rigid-body motions on the deformations of the beam, Eq. (47) may be used to describe the transverse vibrations of the beam. Velocity and acceleration of angular displacement in Eq. (47), $\dot{\alpha}$ and $\ddot{\alpha}$, are determined by the driving torque used to rotate the hub. Such torque can be supplied arbitrarily what we want. For

example, if the value of the torque is invariable with time, then $\dot{\alpha}$ is constant and the hub rotates with a constant speed.

Firstly, we do not consider the effects of rigid-body motions on transverse vibrations of flexible beam, and investigate only using PPF control law to suppress the vibrations of the beam. The general methodology of PPF control is described in Ref. [20]. If the equations describing the structures and actuators are expressed as in the vector case, we have the following model of PPF control:

$$\begin{aligned}\text{System}: \quad & [M]_v\{\ddot{v}\} + [K]_v\{v\} + \dot{\alpha}^2(-[K]_{v1} - [K]_{v2})\{v\} \\ & + \{\ddot{\alpha}[C]_v^{\mathrm{T}}\} = [S]^{\mathrm{T}}[G]\{\eta\},\end{aligned} \tag{49}$$

$$\text{Actuator}: \quad \{\ddot{\eta}\} + 2\xi_f\omega_f\{\dot{\eta}\} + \omega_f^2\{\eta\} = \omega_f^2[S]\{v\}, \tag{50}$$

where $\{\eta\}$ is the filter state vector, $[S]$ the participation matrix, and $[G]$ the gain matrix to be designed. And ξ_f and ω_f are the filter damping ratio and filter frequency, respectively.

MEF control law takes the form [19]

$$\tau(t) = -g_1\alpha - g_2\dot{\alpha} - g_3[(S_0R - M_0) - I_b\ddot{\alpha}], \tag{51}$$

where g_1, g_2 and g_3 are the control gains, and S_0 and M_0 are the root shear force and bending moment of flexible beam, respectively. If employing the coupling of transverse deformations and rigid-body motions of rotating beam system and further adding MEF control on the hub to indirectly suppress transverse vibrations of the beam, Eq. (48) must be included. Substituting Eq. (51) into Eq. (48), the equation can be rewritten as

$$\begin{aligned}&[I_h + I_b + \{v\}^{\mathrm{T}}([K]_{v1} - [K]_{v2})\{v\}]\ddot{\alpha} + 2[\{\dot{v}\}^{\mathrm{T}}([K]_{v1} - [K]_{v2})\{v\}]\dot{\alpha} + [C]_v\{\ddot{v}\} \\ &\quad = -g_1\alpha - g_2\dot{\alpha} - g_3[(S_0R - M_0) - I_b\ddot{\alpha}].\end{aligned} \tag{52}$$

Then, another control modelling, combined PPF and MEF to suppress transverse vibrations of flexible rotating beam, is formed by Eqs. (49), (50) and (52). In such a model, the meaning of torque τ is not the same as that of the model using only PPF control, and law of τ cannot be chosen arbitrarily then. However, as initial drive for rotating the hub, we can still choose the law of the torque as what we expect and that is the reason why rotation speeds of the hub are taken as constant in the following simulations.

Actually, in the process of using PPF and MEF to suppress the transverse vibrations of rotating beam, torque τ must be obtained indirectly from the signals of sensor located at the root of the beam every moment. Such signals include the information of root shear force and bending moment to be used by Eq. (51) to calculate the value of τ. And at the same time, Eq. (52) is applied to determine the angular displacement, speed and acceleration of the hub; all of them will appear in Eq. (49). After that, Eqs. (49) and (50) can be used to implement PPF control for the beam. What should be mentioned here is that there is some extent of time delay in each step of the above processes, because processors need some time to process the signals and apply appropriate signals to the actuator. Of course, the control effect will be better if the time delay is reduced to the least extent.

4.2. Simulation results

To show the benefit of the control scheme of combining the techniques of PPF and MEF, two cases are compared; case 1, only using PPF control (Eqs. (49) and (50)), and case 2, adding control of rigid-body maneuver to case 1 (Eqs. (49), (50) and (52)). The simulations are based on a hub–beam system with physical parameters shown in Table 1. Simulations results for four cases, with different hub rotation speeds $\dot{\alpha} = 0.3$, 1, 3.0 and 4.5 rad/s, are shown in Figs. 3–6, respectively.

The filter parameters ξ_f and ω_f for PPF control are 0.02 and 4.30, respectively, chosen according to the damping ratio and frequency of the first vibrational mode of the non-rotating cantilever beam. The control gain matrix reduces to a constant because only one sensor is located at the root of the beam. Such constant is then selected as 1, the maximum gain value of PPF control. The control gains of MEF for every case are given under each figure.

Table 1
Physical parameters of a hub–beam system to simulation

Beam
Density: $\rho = 2700$ kg/m^3
Young's modulus: $E = 71 \times 10^9$ N/m^2
Width: $b = 10^{-3}$ m
Height: $h = 0.10$ m
Length: $L = 1.10$ m
Cross-sectional area: $A = 10^{-4}$ m^2
Moment of area: $I = 8.33 \times 10^{-12}$ m^4
Hub
Mass moment of inertia: $I_h = 3.84$ kg/m^2
Radius: $R = 0.1$ m

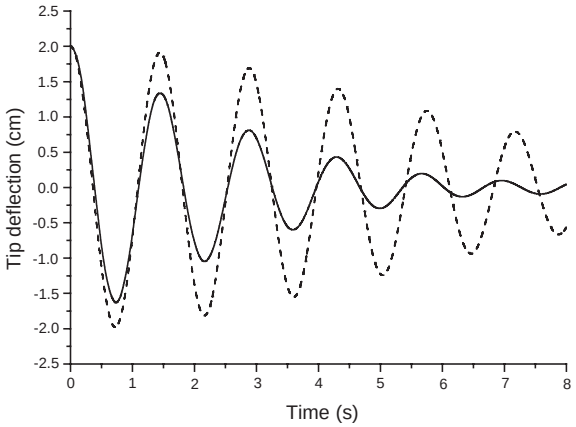

Fig. 3. Tip deflection for $\dot{\alpha} = 0.3$ rad/s: - - - -, case 1, PPF; ——, case 2, PPF and MEF. PPF: $\xi_f = 0.02$, $\omega_f = 4.30$, *gain* = 1.0; MEF: $g_1 = 90$, $g_2 = 30$, $g_3 = 30$.

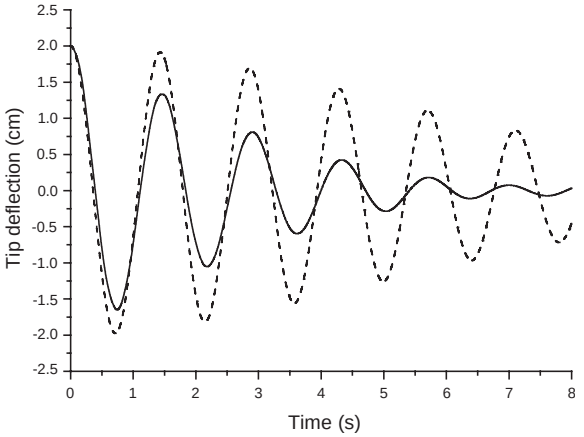

Fig. 4. Tip deflection for $\dot{\alpha} = 1.0$ rad/s: - - - -, case 1, PPF; ——, case 2, PPF and MEF. PPF: $\xi_f = 0.02$, $\omega_f = 4.30$, $gain = 1.0$; MEF: $g_1 = 80$, $g_2 = 25$, $g_3 = 30$.

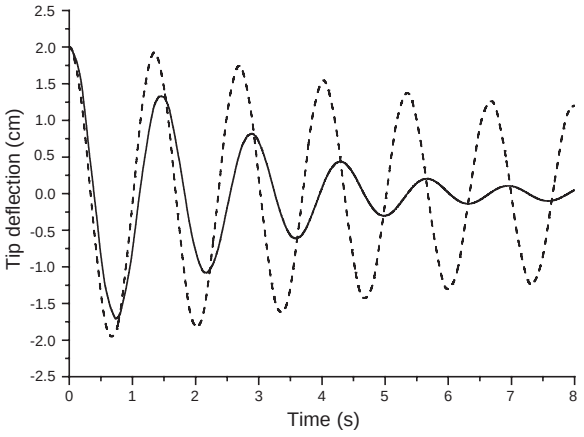

Fig. 5. Tip deflection for $\dot{\alpha} = 3.0$ rad/s: - - - -, case 1, PPF; ——, case 2, PPF and MEF. PPF: $\xi_f = 0.02$, $\omega_f = 4.30$, $gain = 1.0$; MEF: $g_1 = 70$, $g_2 = 25$, $g_3 = 25$.

It is obvious, even though the control gains of PPF are selected as the maximum value 1, performances of suppression are not excellent. And the performances will lower with increasing rotation speeds of the hub. Such a phenomenon arises from the centrifugal stiffening effect. When the hub speed is increased, the effect is also extended, which in turn results in hardening the beam.

The localization of PPF control can be improved by adding MEF on the hub. The numerical results indicate the improvement of case 2 with the inclusion of MEF control, and that the flexible vibrations are dramatically suppressed with PPF and MEF control.

We also can see that the control gains of MEF are decreased as rotation speeds of the hub are increased. The effect of centrifugal stiffening is the right reason for this. The higher the speed the hub rotates, the larger the beam the stiffness. Root shear force and bending moment of the flexible beam will increase with hardening of the beam. Then from Eq. (51), the control gains g_1, g_2 and g_3 can be decreased to some extent. In addition, the relatively unsatisfactory performance of

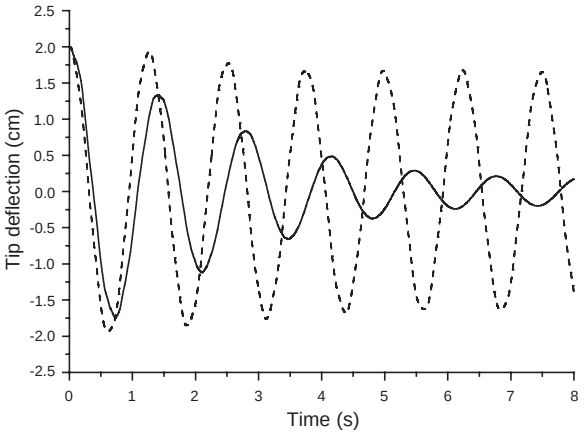

Fig. 6. Tip deflection for $\dot{\alpha} = 4.5$ rad/s: - - - -, case 1, PPF; ——, case 2, PPF and MEF. PPF: $\xi_f = 0.02$, $\omega_f = 4.30$, $gain = 1.0$; MEF: $g_1 = 15$, $g_2 = 15$, $g_3 = 10$.

suppression for the case $\dot{\alpha} = 4.5$ rad/s, when the angular frequency of the rotating hub is above the first natural frequency of transverse vibration of the non-rotating cantilever beam, is also because of the heavily stiffening effect.

5. Conclusions

In this paper, fully coupled non-linear integro-differential equations, describing the axial, transverse and rotational motions of a rotating uniform Euler–Bernoulli beam, are derived by using the extended Hamilton's principle. The centrifugal stiffening effect is taken into account. A finite-dimensional model, including couplings of axial and transverse vibrations, and of elastic deformations and rigid motions, is obtained by the FEM. And by neglecting the axial motion, a simplified FEM model is used to study suppression of transverse vibrations of a rotating beam with PPF and MEF control simultaneously. It is indicated that excellent performance can be achieved with this scheme.

Acknowledgements

The authors gratefully acknowledge the support from the National Natural Science Foundation of China.

References

[1] A. Yigit, R.A. Scott, A.G. Ulsoy, Flexural motion of a rotating beam attached to a rigid body, *Journal of Sound and Vibration* 121 (1988) 201–210.

[2] G. Naganathan, A.H. Soni, Coupling effects of kinematics and flexibility in manipulators, *The International Journal of Robotics Research* 6 (1987) 75–85.

[3] S. Hunagud, S. Sarkar, Problem of the dynamics of a cantilever beam attached to a moving base, *Journal of Guidance, Control, and Dynamics* 12 (1989) 438–441.
[4] H. Baruh, S.S.K. Tadikonda, Issues in dynamics and control of flexible robot manipulators, *Journal of Guidance, Control, and Dynamics* 12 (1989) 569–671.
[5] S. Choura, S. Jayasuriya, M.A. Medick, On the modeling, and open-loop control of a rotating thin flexible beam, *Transactions of the American Society of Mechanical Engineers, Journal of Dynamic Systems, Measurement, and Control* 113 (1991) 26–33.
[6] T.R. Kane, R.R. Ryan, A.K. Bannerjee, Dynamics of a cantilever beam attached to a moving base, *Journal of Guidance, Control, and Dynamics* 10 (1987) 139–151.
[7] J.C. Simo, L. Vu-Quoc, On the dynamics of a flexible beams under large overall motions—the plane case: part II, *Transactions of the American Society of Mechanical Engineers, Journal of Applied Mechanics* 53 (1986) 855–863.
[8] J.C. Simo, L. Vu-Quoc, The role of nonlinear theories in transient analysis of flexible structure, *Journal of Sound and Vibration* 119 (1987) 487–508.
[9] A.M. Bloch, Stability analysis of a rotating flexible system, *Acta Applicandae Mathematicae* 15 (1989) 211–234.
[10] W.D. Zhu, C.D. Mote Jr., Dynamics modeling and optimal control of rotating Euler–Bernoulli beams, *Transactions of the American Society of Mechanical Engineers, Journal of Dynamic Systems, Measurement, and Control* 119 (1997) 802–808.
[11] K. Yuan, C.-M. Hu, Nonlinear modeling and partial linearizing control of a slewing Timoshenko-beam, *Transactions of the American Society of Mechanical Engineers, Journal of Dynamic Systems, Measurement, and Control* 118 (1996) 75–83.
[12] S. Putter, H. Manor, Natural frequencies of radial rotating beams, *Journal of Sound and Vibration* 56 (1978) 175–185.
[13] S.V. Hoa, Vibration of a rotating beam with tip mass, *Journal of Sound and Vibration* 67 (1979) 369–381.
[14] Y.A. Khulief, Vibration frequencies of a rotating tapered beam with end mass, *Journal of Sound and Vibration* 134 (1989) 87–97.
[15] A.D. Wright, G.E. Smith, R.W. Thresher, J.C.L. Wang, Vibration modes of centrifugally stiffened beams, *Journal of Applied Mechanics* 49 (1982) 197–202.
[16] H. Du, M.K. Lim, K.M. Liew, A power solution for vibration of a rotating Timoshenko beam, *Journal of Sound and Vibration* 175 (1994) 505–523.
[17] Z.H. Luo, B.Z. Guo, Shear force feedback control of a single link flexible robot with a revolute joint, *IEEE Transactions on Automatic Control* 42 (1997) 53–65.
[18] S.B. Choi, C.C. Cheong, H.C. Shin, Sliding mode control of vibration in a single-link flexible arm with parameter vibrations, *Journal of Sound and Vibration* 179 (1995) 737–748.
[19] Z. Li, P.M. Bainum, Momentum exchange: feedback control of flexible spacecraft maneuvers and vibration, *Journal of Guidance, Control, and Dynamics* 15 (1992) 1354–1360.
[20] C.J. Goh, T.K. Caughey, On the stability problem caused by finite actuator dynamics in the collocated control of large space structures, *International Journal of Control* 41 (1985) 787–802.
[21] M. Stylianou, B. Tabarrok, Finite element analysis of an axially moving beam part I: time integration, *Journal of Sound and Vibration* 178 (1994) 433–453.
[22] L. Meriovitch, *Analytical Methods in Vibrations*, Macmillan, New York, 1967.